ORIGINAL RESEARCH

Prognostic Factors for Patients with Proliferative Hepatocellular Carcinoma After Liver Resection

Hong-Mei Li[*], Wei Huang [ID][*], Chao Hu, Zi-Shu Zhang, Yu-Dong Xiao [ID], Tian-Cheng Wang [ID]

Department of Radiology, the Second Xiangya Hospital of Central South University, Changsha, People's Republic of China

*These authors contributed equally to this work

Correspondence: Tian-Cheng Wang; Yu-Dong Xiao, Tel +8613637403027, Fax +86 0731-85533525, Email wangtiancheng94@csu.edu.cn; xiaoyudong222@csu.edu.cn

Purpose: There is a scarcity of predictive models currently accessible for prognosticating proliferative hepatocellular carcinoma (HCC), an integrated class of subtype, characterized by a dismal prognosis. Consequently, this study aimed to develop and validate a novel prognostic model capable of accurately predicting the prognosis of proliferative HCC after curative resection.

Patients and Methods: This retrospective multicenter study included patients with solitary HCC who underwent curative liver resection from August 2014 to December 2020 (n = 816). Patients were stratified into either the proliferative HCC cohort (n = 259) or the nonproliferative HCC cohort (n = 557) based on histological criteria. Disease-free survival (DFS) was compared between the two groups before and after one-to-one propensity score matching (PSM). Of all the proliferative HCC patients, 203 patients were assigned to training cohort, and 56 patients were assigned to validation cohort. Univariate and multivariate analyses were performed in training cohort to identify risk factors associated with worse DFS. Thereafter, a predictive model was constructed, subsequently validated in the validation cohort.

Results: The DFS of proliferative HCC was significantly worse than nonproliferative HCC before and after PSM. Meanwhile, multivariate regression analysis revealed that liver cirrhosis (P = 0.032) and larger tumor size (P = 0.000) were independent risk factors of worse DFS. Lastly, the discriminative abilities of the predictive model for 1, 3, 5-year DFS rates, as determined by receiver operating characteristic (ROC) curves, were 0.702, 0.720, and 0.809 in the training cohort and 0.752, 0.776, and 0.851 in the validation cohort, respectively.

Conclusion: This study developed a predictive model with satisfactory accuracy to predict the worse DFS in proliferative HCCs after liver resection. Moreover, this predictive model may serve as a valuable tool for clinicians to predict postoperative HCC recurrence, thereby enabling them to implement early preventative strategies.

Keywords: hepatocellular carcinoma, proliferative, nonproliferative, predictive model, curative resection

Introduction

Hepatocellular carcinoma (HCC) can be classified into proliferative and nonproliferative categories based on their molecular and histological characteristics.[1] Proliferative HCCs, which account for 30–50% of all HCCs, encompass a diverse group of tumors with aggressive biological features, including various histological subtypes such as scirrhous, macrotrabecular-massive (MTM), sarcomatoid, and neutrophil-rich HCCs. Additionally, the progenitor subtype, hallmarked by the presence of cytokeratin 19 (CK19), is considered part of the proliferative type despite not being a true histological subtype.[1–3] To date, surgical resection remains the primary curative treatment modality for HCCs and is extensively endorsed in various guidelines.[4–6] Given the elevated malignancy level of proliferative HCCs, the post-resection prognosis of proliferative HCCs is unfavorable, and recurrence rates are relatively high. As demonstrated by Kang et al, proliferative HCCs have worse prognostic outcomes following liver resection compared to nonproliferative HCCs.[2] Consequently, accurate prediction of proliferative HCC recurrence holds significant implications for improving prognosis.

To date, numerous staging systems have been employed to assess the prognosis of HCC following liver resection.[7–11] However, compelling evidence suggests that proliferative HCCs behave differently from nonproliferative HCCs, with distinct prognoses and prognostic factors.[1,2,12–16] As mentioned by Kang et al, proliferative HCC is an independent factor for poor over-all survival, higher rate of intrahepatic distant recurrence, and extrahepatic metastasis after curative surgery. In addition, rim arterial phase hyperenhancement at gadoxetate-enhanced MRI was independent predictors for proliferative HCC and poor prognosis.[2] Attributable to the rarity of proliferative HCCs, there is a paucity of predictive models or staging systems for assessing its prognosis after liver resection. Therefore, there is an urgent need to generate a predictive model for proliferative HCCs to stratify their prognosis and improve clinical management strategies. The nomogram is a clinical predictive model derived from multivariate regression analysis, enabling the incorporation of multiple predictors for improved prognostic evaluation. Moreover, the nomogram possesses the capability to tailor the calculation of an individual's disease-free survival (DFS) or overall survival (OS) thereby demonstrating its clinical applicability.

Therefore, the current study aimed to develop and validate a prognostic prediction model using a nomogram from a cohort of proliferative HCC patients who underwent liver resection.

Patients and Methods
Study Population
This retrospective study was conducted at multiple centers (three tertiary referral hospitals). HCC patients who underwent liver resection as the primary treatment from August 2014 to December 2020 were eligible to participate in this study. The inclusion criteria were as follows: 1) solitary tumor; 2) Child-Pugh class A or B; 3) absence of vascular invasion or extrahepatic metastasis. The exclusion criteria were as follows: 1) failure to achieve R0 resection of HCC; 2) absence of baseline CT imaging within 1 month prior to surgery; 3) unavailable baseline laboratory test results within 1 week before surgery; 4) absence of follow-up data. A total of 816 HCC patients were enrolled in this study, with 636 participants from institution A and 180 participants from institutions B and C. The study process flowchart is illustrated in Figure 1. The study was approved by the institutional review boards of the Second Xiangya Hospital of Central South University, the Affiliated Cancer Hospital of Guizhou Medical University, and the Affiliated Hospital of Guizhou Medical University. This study was conducted in accordance with the Helsinki Declaration. As the study was retrospective and patient data was anonymized and de-identified prior to analysis, the requirement for written consent was waived.

Data Collection
Clinical data collected comprised age, sex, etiology of liver disease, and presence of cirrhosis. Imaging features included the diameter of the largest tumor, the shape of the tumor, the presence of satellite nodules, and the presence of portal hypertension. Laboratory parameters included neutrophil count, lymphocyte count, platelet count, and systemic immune-inflammation index (SII), as well as serum albumin levels, total bilirubin levels, albumin-bilirubin (ALBI) grade, and alpha-fetoprotein (AFP) levels. A prior study identified that SII > 330 was an independent risk factor for the prognosis of HCC patients undergoing liver resection.[17] Therefore, 330 was selected as the cutoff value of SII in the present study. The timing of preoperative imaging examinations and surgical procedures was also documented. Liver cirrhosis was diagnosed by histopathological biopsy and was defined as an advanced form of progressive hepatic fibrosis with distortion of the hepatic architecture and regenerative nodule formation.[18] The diameter of the largest tumor, the shape of the tumor, and the presence of satellite nodules were recorded accordingly.[19] Measurement of portal vein pressure was not routinely performed in these three institutions; therefore, portal hypertension was defined as the presence of at least two of the following findings: varices, ascites, or splenomegaly on imaging results.[20,21] Splenomegaly was assessed by CT scans and defined as a spleen size with any axis >12 cm, or a transverse dimension exceeding 5 rib spaces, or a visible spleen below the level of the liver edge.
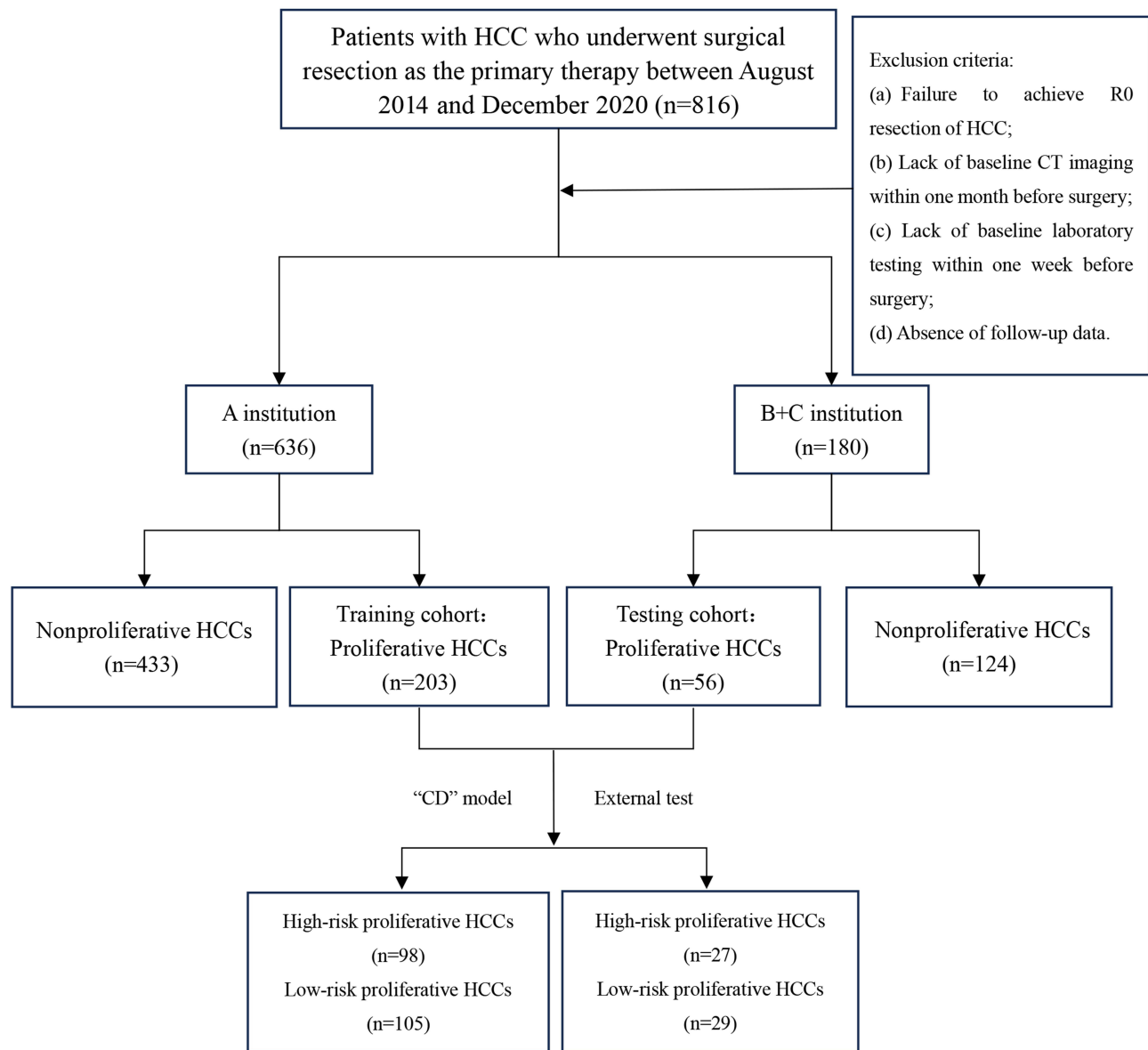
Figure 1 Study flowchart. Patients with proliferative hepatocellular carcinoma who underwent liver resection in institution (**A**) (n=203) were included in the training cohort for establishing the predictive model. Patients from institutions (**B** and **C**) (n=56) were included in the external validation cohort.

Histological Analysis

An experienced pathologist (with more than 10 years of experience in hepatic pathology) reviewed the pathological slides of all resected hepatocellular carcinomas to determine the histological subtypes of HCC. The histomorphology subtype of HCC was classified in accordance with the 2019 WHO classification.[22] CK19 immunohistochemistry was also performed on all representative whole-tissue HCC sections. HCC expressing CK19 in more than 5% of tumor cells was categorized as proliferative HCC, whilst CK19-negative HCC was defined as either unstained by immunohistochemistry or expressing CK19 in less than 5% of tumor cells. Besides, MTM, neutrophil-rich, scirrhous, sarcomatoid, and CK19-positive conventional HCC were categorized as proliferative HCC, whereas steatohepatitic, clear cell, lymphocyte-rich, and CK19-negative conventional HCC were designated nonproliferative HCC.[1–3,16]

Follow-Up Evaluation and Endpoints

All patients underwent clinical and radiological follow-up assessments. The latter included ultrasound every 2–3 months during the first year after surgery, and at least every 6 months thereafter. When suspicious recurrence was detected in the liver, further evaluation was performed using at least two imaging modalities (contrast enhanced CT or MRI).[18]F-fluorodeoxyglucose (^{18}F-FDG) PET scan, brain CT or MRI, or bone scan was performed in case of symptomatic brain or bone metastases. Additionally, routine blood tests, including complete blood count, liver function, and serum AFP measurement were routinely conducted for surveilling recurrence.

The endpoint of this study was DFS, defined as the time from the date of surgery to HCC recurrence or death from any cause, as determined by the last hospital or telephone follow-up. If tumor recurrence occurred, treatment options such as ablation, repeat surgery, transarterial chemoembolization (TACE), or liver transplantation were performed based on the patient's condition, tumor location, and size.

Statistical Analysis

Continuous variables were expressed as median and interquartile range, whereas categorical variables were presented as frequency and proportion. The *t*-test and chi-square test were used to assess differences between the training and validation cohorts. The Cox proportional hazards model was used to establish the predictive model based on the DFS and variables in the training cohort. The univariate and multivariate regression method was used to identify independent predictors of worse DFS, which were expressed as hazard ratio (HR), 95% confidence intervals (CI), and p-value.

The predictive performance of the nomogram was evaluated by the area under the receiver operating characteristic curve (AUC) in the training and validation cohorts. Based on the nomogram of the final model, a risk score for postoperative proliferative HCC was obtained. The optimal cutoff point for the risk score was determined by Kaplan–Meier curve. Proliferative HCC was classified into risk groups based on the risk score and subgroup analysis was then conducted. The DFS was analyzed using the Kaplan–Meier curve both in training and testing cohorts, and the Log rank test was used for significance testing. In addition, the DFS was compared among high risk proliferative, low risk proliferative, and nonproliferative HCC in the entire cohort as well as in institution A, and institutions B+C.

Statistical analyses were performed using SPSS statistical software (SPSS version 25, International Business Machines Corporation) and R software (version 4.3.0, http://www.R-project.org). P < 0.05 was considered statistically significant.

Results
Baseline Characteristics of the Study Population

A total of 816 patients were included in this study, with 259 categorized as proliferative HCC and 557 as nonproliferative HCC. Among the proliferative HCC cases, 203 (78.4%, 203/259) patients were from institution A (66 cases of MTM, 31 scirrhous, 3 cases of sarcomatoid, 4 cases of neutrophil-rich, and 99 cases of CK19 positive conventional HCC), serving as the training cohort for developing the prognostic model. Fifty-six patients (21.6%, 56/259) were from institutions B and C (22 cases of MTM, 11 cases of scirrhous, 1 case of sarcomatoid, and 22 cases of CK 19 positive conventional HCC), serving as the external validation cohort for testing the prognostic model. Among the nonproliferative HCC cases, 433 patients were from institution A (13 cases of steatohepatitic, 6 cases of lymphocyte-rich, 9 cases of clear cell, and 405 cases of CK19 negative conventional HCC), and 124 patients were from institutions B and C (1 case of steatohepatitic, 1 case of lymphocyte-rich, 11 cases of clear cell, and 111 cases of CK19 negative conventional HCC). The baseline characteristics of patients in the training and validation cohorts are listed in Table 1. The imaging features and pathological characteristics are displayed in Figure 2A and B.

Comparison of DFS Between Proliferative and Nonproliferative HCC

Compared to the nonproliferative HCC group, patients in the proliferative HCC group exhibited a lobulated tumor shape, higher AFP levels, presence of satellite nodules, larger tumors, and higher SII level (Table 2). Kaplan–Meier survival

Table I The Demographic, Radiological and Laboratorial Characteristics of Patients in Training Cohort and Validation Cohort

Baseline Characteristics	Total (n = 259)	Training Cohort (n = 203)	Testing Cohort (n = 56)	P
Sex, n (%)				0.934
Male	216 (83)	170 (84)	46 (82)	
Female	43 (17)	33 (16)	10 (18)	
Age (y), n (%)				< 0.001
≤55	145 (56)	128 (63)	17 (30)	
>55	114 (44)	75 (37)	39 (70)	
Portal hypertension, n (%)				0.905
Absent	209 (81)	163 (80)	46 (82)	
Present	50 (19)	40 (20)	10 (18)	
Child-Pugh class, n (%)				0.260
A	240 (93)	190 (94)	50 (89)	
B	19 (7)	13 (6)	6 (11)	
Etiology of Liver disease, n (%)				0.391
None	45 (17)	34 (17)	11 (20)	
HBV	193 (75)	150 (74)	43 (77)	
Other	21 (8)	19 (9)	2 (4)	
Cirrhosis, n (%)				0.696
Absent	112 (43)	86 (42)	26 (46)	
Present	147 (57)	117 (58)	30 (54)	
Shape of the tumor, n (%)				0.521
Round	122 (47)	93 (46)	29 (52)	
Lobulated	137 (53)	110 (54)	27 (48)	
Satellite nodule, n (%)				0.018
Absent	222 (86)	168 (83)	54 (96)	
Present	37 (14)	35 (17)	2 (4)	
AFP (ng/mL), n (%)				0.601
≤200	112 (43)	90 (44)	22 (39)	
>200	147 (57)	113 (56)	34 (61)	
Diameter of the largest tumor (mm), n (%)				1.000
≤50	134 (52)	105 (52)	29 (52)	
>50	125 (48)	98 (48)	27 (48)	
Neutrophil count (×10^9/L), Median (Q1, Q3)	3.7 (2.6, 4.6)	3.7 (2.8, 4.6)	3.4 (2.4, 4.1)	0.055
Lymphocyte count (×10^9/L), Median (Q1, Q3)	1.3 (1.0, 1.6)	1.3 (1.0, 1.6)	1.3 (1.0, 1.7)	0.885
Platelet count (×10^9/L), Median (Q1, Q3)	167.0 (121.5, 223.0)	165.0 (123.0, 222.5)	178.5 (111.8, 224.8)	0.816
SII, n (%)				0.411
≤330	92 (36)	69 (34)	23 (41)	
>330	167 (64)	134 (66)	33 (59)	
Serum albumin (g/L), Median (Q1, Q3)	39.1 (36.0, 42.4)	38.9 (35.9, 42.2)	40.8 (37.3, 43.3)	0.016
Total bilirubin (mg/dL), Median (Q1, Q3)	14.3 (10.1, 19.2)	14.5 (10.7, 19.3)	13.4 (9.2, 18.1)	0.183
ALBI grade, n (%)				0.015
1	125 (48)	89 (44)	36 (64)	
2	133 (51)	113 (56)	20 (36)	
3	1 (0)	1 (0)	0 (0)	

Abbreviations: AFP, alpha-fetoprotein; SII, systemic immune-inflammation index; ALBI, albumin-bilirubin.

curves of DFS in patients with proliferative HCC group and nonproliferative HCC are delineated in Figure 3. Compared to those in the proliferative HCC group, patients in the nonproliferative HCC group had a significantly better DFS (nonproliferative HCC, 27.4 months [IQR, 10.7–44.7] vs proliferative HCC, 10.9 months [IQR, 3.6–30.2]; p < 0.001)
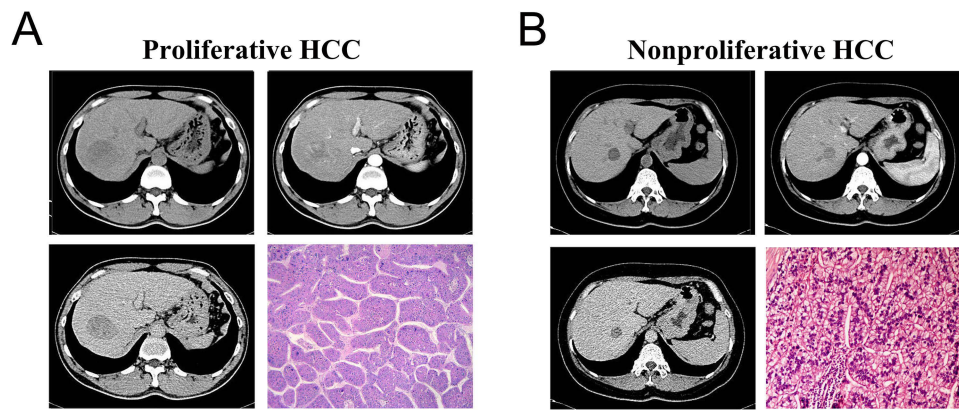
Figure 2 (**A**) Images showing a case of proliferative hepatocellular carcinoma in the 7th segment of the liver of a 50-year-old man with cirrhosis. The lesion was 41 mm in size, with an oval shape, and without satellite nodules on the CT images. CT image during the arterial phase displayed heterogenous enhancement. A washout appearance was observed in the delayed phase of the CT scan. These observations qualified as Liver Imaging Reporting and Data System category 5. Microscopic examination with hematoxylin and eosin staining confirmed the presence of the macrotrabecular-massive HCC subtype. (**B**) Images illustrating a case of nonproliferative hepatocellular carcinoma at the junction of the 7th and 8th segments of the liver of a 48-year-old woman without cirrhosis. The lesion was 22 mm in size, with a round shape, and without satellite nodules on the CT images. CT image during the arterial phase CT image showed moderate enhancement, while a washout appearance was noted during the delayed phase. These observations qualified as Liver Imaging Reporting and Data System category 5. Microscopic examination with hematoxylin and eosin staining confirmed the presence of the clear cell HCC subtype.

(Table 2 and Figure 3A). Moreover, to mitigate the risk of selection bias originating from confounding factors between the two groups, a one-to-one PSM analysis was performed. After PSM, 398 patients were enrolled, of which 199 cases were proliferative HCC and 199 cases were nonproliferative HCC. The baseline characteristics were comparable between the two groups after PSM (Table 3), which showed no statistical difference between baseline characteristics. In line with

Table 2 The Baseline Characteristics of Proliferative and Nonproliferative HCC Before PSM in the Entire Population

Baseline Characteristics	Total (n = 816)	Nonproliferative HCC (n = 557)	Proliferative HCC (n = 259)	P
DFS (m), Median (Q1, Q3)	24.3 (6.6, 43.3)	27.4 (10.7, 47.7)	10.9 (3.6, 30.2)	< 0.001
Sex, n (%)				0.799
Male	686 (84)	470 (84)	216 (83)	
Female	130 (16)	87 (16)	43 (17)	
Age (y), n (%)				0.382
≤55	437 (54)	292 (52)	145 (56)	
>55	379 (46)	265 (48)	114 (44)	
Portal hypertension, n (%)				0.862
Absent	654 (80)	445 (80)	209 (81)	
Present	162 (20)	112 (20)	50 (19)	
Child-Pugh class, n (%)				0.681
A	762 (93)	522 (94)	240 (93)	
B	54 (7)	35 (6)	19 (7)	
Etiology of Liver disease, n (%)				0.151
None	164 (20)	119 (21)	45 (17)	
HBV	571 (70)	378 (68)	193 (75)	
Other	81 (10)	60 (11)	21 (8)	
Cirrhosis, n (%)				0.302
Absent	376 (46)	264 (47)	112 (43)	
Present	440 (54)	293 (53)	147 (57)	
Shape of the tumor, n (%)				< 0.001
Round	557 (68)	435 (78)	122 (47)	
Lobulated	259 (32)	122 (22)	137 (53)	

(*Continued*)

Table 2 (Continued).

Baseline Characteristics	Total (n = 816)	Nonproliferative HCC (n = 557)	Proliferative HCC (n = 259)	P
Satellite nodule, n (%)				< 0.001
Absent	758 (93)	536 (96)	222 (86)	
Present	58 (7)	21 (4)	37 (14)	
AFP (ng/mL), n (%)				< 0.001
≤200	494 (61)	382 (69)	112 (43)	
>200	322 (39)	175 (31)	147 (57)	
Diameter of the largest tumor (mm), n (%)				0.004
≤50	483 (59)	349 (63)	134 (52)	
>50	333 (41)	208 (37)	125 (48)	
Neutrophil count (×10^9/L), Median (Q1, Q3)	3.3 (2.4, 4.3)	3.1 (2.3, 4.1)	3.7 (2.6, 4.6)	< 0.001
Lymphocyte count (×10^9/L), Median (Q1, Q3)	1.3 (1.0, 1.7)	1.3 (1.0, 1.8)	1.3 (1.0, 1.6)	0.131
Platelet count (×10^9/L), Median (Q1, Q3)	155 (108.0, 209.3)	147 (101.0, 202.0)	167 (121.5, 223.0)	< 0.001
SII, n (%)				< 0.001
≤330	387 (47)	295 (53)	92 (36)	
>330	429 (53)	262 (47)	167 (64)	
Serum albumin (g/L), Median (Q1, Q3)	39.1 (36.3, 42.2)	39.1 (36.5, 42.0)	39.1 (36.0, 42.4)	0.949
Total bilirubin (mg/dL), Median (Q1, Q3)	13.8 (10.2, 18.9)	13.4 (10.2, 18.7)	14.3 (10.1, 19.2)	0.430
ALBI grade, n (%)				0.616
1	396 (49)	271 (49)	125 (48)	
2	412 (50)	279 (50)	133 (51)	
3	8 (1)	7 (1)	1 (0)	

Abbreviations: HCC, hepatocellular carcinoma; DFS, disease free survival; AFP, alpha-fetoprotein; SII, systemic immune-inflammation index; ALBI, albumin-bilirubin.

the above results, compared to the proliferative HCC group, patients in the nonproliferative HCC group had a significantly better DFS (nonproliferative HCC, 26.0 months [IQR, 6.8–41.7] vs proliferative HCC, 12.0 months [IQR, 4.2–30.0]; p = 0.001) (Table 3 and Figure 3B).
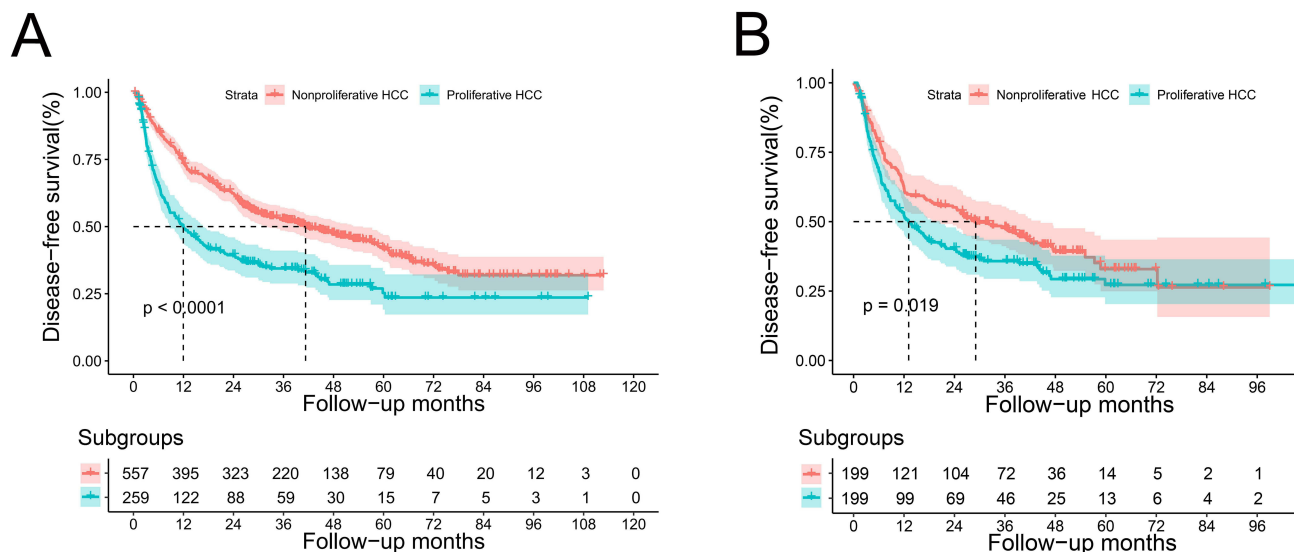

Figure 3 Disease-free survival curves of proliferative and nonproliferative HCC before (**A**) and after (**B**) propensity score matching in the entire cohort.

Table 3 The Baseline Characteristics of Proliferative and Nonproliferative HCC After PSM in the Entire Population

Baseline characteristics	Total (n = 398)	Nonproliferative HCC (n = 199)	Proliferative HCC (n = 199)	p
DFS (m), Median (Q1, Q3)	16.3 (5.3, 39.5)	26.0 (6.8, 41.7)	12.0 (4.2, 30.0)	0.001
Sex, n (%)				1.000
Male	334 (84)	167 (84)	167 (84)	
Female	64 (16)	32 (16)	32 (16)	
Age (y), n (%)				1.000
≤55	227 (57)	113 (57)	114 (57)	
>55	171 (43)	86 (43)	85 (43)	
Portal hypertension, n (%)				1.000
Absent	317 (80)	158 (79)	159 (80)	
Present	81 (20)	41 (21)	40 (20)	
Child-Pugh class, n (%)				1.000
A	372 (93)	186 (93)	186 (93)	
B	26 (7)	13 (7)	13 (7)	
Etiology of Liver disease, n (%)				0.851
None	78 (20)	41 (21)	37 (19)	
HBV	287 (72)	141 (71)	146 (73)	
Other	33 (8)	17 (9)	16 (8)	
Cirrhosis, n (%)				0.920
Absent	180 (45)	89 (45)	91 (46)	
Present	218 (55)	110 (55)	108 (54)	
Shape of the tumor, n (%)				0.919
Round	228 (57)	115 (58)	113 (57)	
Lobulated	170 (43)	84 (42)	86 (43)	
Satellite nodule, n (%)				0.654
Absent	377 (95)	190 (95)	187 (94)	
Present	21 (5)	9 (5)	12 (6)	
AFP (ng/mL), n (%)				0.763
≤200	190 (48)	93 (47)	97 (49)	
>200	208 (52)	106 (53)	102 (51)	
Diameter of the largest tumor (mm), n (%)				0.762
≤50	222 (56)	113 (57)	109 (55)	
>50	176 (44)	86 (43)	90 (45)	
Neutrophil count (×10^9/L), Median (Q1, Q3)	3.5 (2.5, 4.5)	3.3 (2.5, 4.6)	3.6 (2.6, 4.4)	0.544
Lymphocyte count (×10^9/L), Median (Q1, Q3)	1.3 (1.0, 1.6)	1.2 (1.0, 1.7)	1.3 (1.0, 1.6)	0.711
Platelet count (×10^9/L), Median (Q1, Q3)	165.5 (110.3, 223.0)	166.0 (107.0, 228.0)	165.0 (115.5, 221.0)	0.961
SII, n (%)				1.000
≤330	152 (38)	76 (38)	76 (38)	
>330	246 (62)	123 (62)	123 (62)	
Serum albumin (g/L), Median (Q1, Q3)	39.6 (36.3, 42.6)	39.7 (36.6, 42.5)	39.4 (36.2, 42.9)	0.945
Total bilirubin (mg/dL), Median (Q1, Q3)	13.9 (10.1, 18.4)	13.1 (10.0, 17.1)	14.6 (10.1, 19.3)	0.082
ALBI grade, n (%)				0.291
1	205 (52)	106 (53)	99 (50)	
2	191 (48)	91 (46)	100 (50)	
3	2 (1)	2 (1)	0 (0)	

Abbreviations: HCC, hepatocellular carcinoma; DFS, disease free survival; AFP, alpha-fetoprotein; SII, systemic immune-inflammation index; ALBI, albumin-bilirubin.

Potential Predictive Factors for the Prognosis of Proliferative HCC

Significant predictors of DFS in the univariate analysis (P ≤ 0.100) comprised the diameter of the largest tumor (P = 0.000), SII (P = 0.010), satellite nodule (P = 0.023), shape of the tumor (P = 0.027), and cirrhosis (P = 0.100). Thereafter, these variables were incorporated into the multivariate Cox regression model, and the results

demonstrated that independent risk factors for worse DFS were a tumor diameter larger than 50 mm (HR2.21; 95% CI 1.53–3.20; P = 0.000) and the presence of cirrhosis (HR 1.47; 95% CI 1.03–2.08; P = 0.032) (Table 4).

Development and Validation of the Predictive Model

Based on the independent risk factors identified by multivariable Cox regression analysis, a predictive model for proliferative HCC following surgical resection was constructed and labeled the "CD" model. "C" represents cirrhosis, and "D" represents diameter of the largest tumor. The determination coefficient (R^2) of this model was 0.139, whilst the Likelihood Ratio chi-square value was 30.36. As anticipated, this prognostic model could successfully divide proliferative HCC into two subgroups, with the optimal cutoff value being 35.99. Accordingly, patients were stratified into a low-risk subgroup and a high-risk subgroup of proliferative HCC. In the training cohort, 105 patients (51.7%) were classified as low-risk proliferative HCC, with 1-, 3-, and 5-year DFS rates of 66.4%, 48.1%, and 38.5%. Ninety-eight (48.3%) patients were classified as high-risk proliferative HCC with 1-, 3-, and 5-year DFS rates of 32.5%, 17.4%, and 15.3%. In the validation cohort, twenty-nine patients (51.8%) were classified as low-risk proliferative HCC, with respective 1-, 3-, and 5-year DFS rates of 66.7%, 54.0%, and 35.4%. Twenty-seven patients (48.2%) were classified as high-risk proliferative HCC, with 1- and 3-year DFS rates of 27.1% and 16.3%.

The predictive nomogram is portrayed in Figure 4A. The discriminative abilities of the predictive model for 1-, 3- and 5-year DFS, as determined by ROC curves, were 0.702, 0.720, and 0.809 in the training cohort (Figure 4B) and 0.752, 0.776, 0.851 in the validation cohort, respectively (Figure 4C). Of note, the low-risk proliferative HCC subgroup had significantly better DFS compared to the high-risk subgroup in both the training and validation cohorts (Figure 5).

Comparison of DFS Between High/Low Risk Proliferative and Nonproliferative HCC

Subsequently, the DFS was compared among the high-risk proliferative HCC group, low-risk proliferative HCC group, and nonproliferative HCC group. As depicted in Figures 6A–C, there was no difference in DFS between low-risk proliferative HCC and nonproliferative HCC in the total cohort, institution A cohort, and institution B+C cohorts. However, compared to patients in the low-risk proliferative HCC and nonproliferative HCC cohorts, those in the high-risk proliferative HCC cohort displayed a worse DFS (P < 0.001) in the total cohort, institution A cohort, and institution B+C cohorts.

Table 4 Assessment of Potential Risk Factors for Postoperative Prognosis of Proliferative HCC in Training Cohort

Variables	Univariable Analysis		Multivariable Analysis	
	Hazard Ratio	**95% CI**	**Hazard Ratio**	**95% CI**
Sex	0.84	0.52–1.35		
Age	1.02	0.72–1.45		
Portal hypertension	1.00	0.65–1.53		
Splenomegaly	1.13	0.81–1.59		
Etiology of Liver disease	1.21	0.88–1.68		
Cirrhosis	1.34	0.95–1.89	1.47	1.03–2.08
Shape of the tumor	1.47	1.04–2.07		
Satellite nodule	1.62	1.07–2.47		
AFP	1.07	0.76–1.51		
Diameter of the largest tumor	2.50	1.76–3.53	2.21	1.53–3.20
SII	1.63	1.12–2.38		
ALBI grade	1.28	0.92–1.78		

Abbreviations: AFP, alpha-fetoprotein; SII, systemic immune-inflammation index; ALBI, albumin-bilirubin; CI, confidence interval.
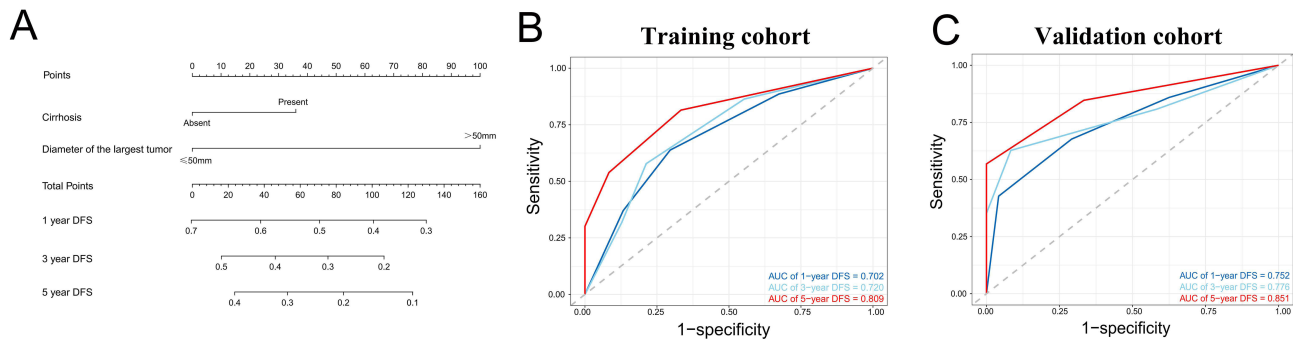
Figure 4 (**A**) Nomogram for predicting the probability of disease-free survival at 1, 3, and 5 years. Each predictor corresponds to a specific point by drawing a line straight upward to the points axis. The sum of the points is located on the total points axis, and this sum represents the probability of disease-free survival. (**B**) ROC curves in the training cohort. (**C**) ROC curves in the validation cohort.
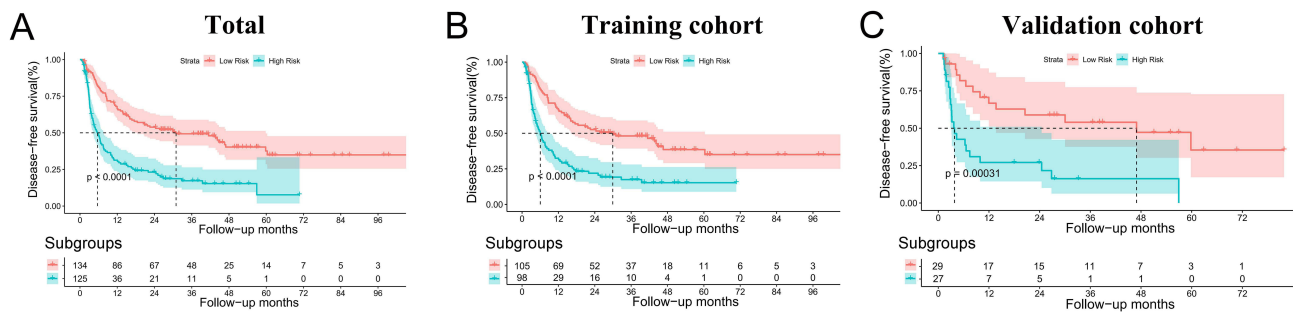

Figure 5 Disease-free survival curves for the total cohort (**A**), training cohort (**B**), and validation cohort (**C**).
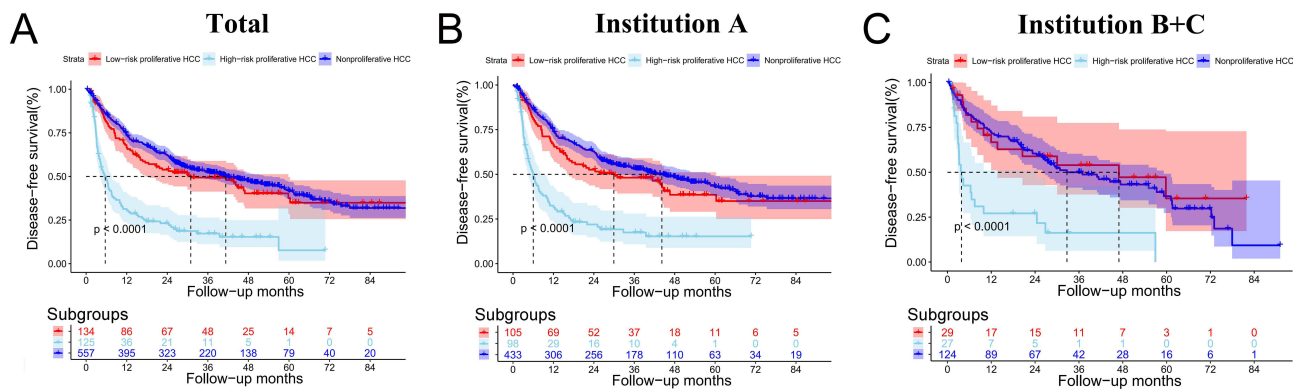
Figure 6 Survival curves of the nonproliferative, high-risk proliferative, and low-risk proliferative hepatocellular carcinoma in the total cohort (**A**), institution A (**B**), and institution B+C (**C**).

Discussion

As is well documented, proliferative HCCs generally present a more unfavorable prognosis in comparison to nonproliferative HCCs. Indeed, the recurrence rate of the former in patients undergoing liver resection is extremely high, and prognosis can vary even among patients with the same clinical stage.[1–3,12–15,23,24] Therefore, preoperative or postoperative prognostic stratification is crucial for treatment decision-making. To date, several models, such as the Korean model, SLICER, and SSCLIP, have been specifically designed to predict the prognosis of HCC after liver resection.[7–11,19] However, the prognostic prediction models for proliferative HCC undergoing liver resection remain limited.

In the present study, the DFS of proliferative HCC was significantly worse than that of nonproliferative HCC before and after PSM analysis. Subsequently, a prognostic prediction model was developed and validated using a nomogram for proliferative HCC. It is worthwhile pointing out that our predictive model had satisfactory prognostic ability in both the training and validation cohorts and enabled a personalized evaluation of the prognosis of patients with proliferative HCCs undergoing liver resection. The results signaled that liver cirrhosis and larger tumor sizes were significantly associated with worse DFS. The first independent predictor for a poor prognosis in proliferative HCC patients is liver cirrhosis. Liu et al reported that liver cirrhosis is one of the hallmarks of proliferative HCC, and the progression of proliferative HCC may be facilitated by liver cirrhosis through the formation of a collagen-rich, inflexible pathway that promotes the migration of cancer cells.[25] In addition, earlier studies concluded that cirrhotic livers generate immune-mediated cancer fields, as evidenced by multiple gene signatures derived from cirrhotic liver tissues, which is conducive to the progression of HCC.[26–29] Larger tumor size is another independent predictor for a poor prognosis in proliferative HCC. Larger tumors have been reported to exhibit greater intratumoral heterogeneity, resulting in a higher risk of drug resistance and a worse prognosis.[24,30] Consistent with the observations of previous studies, our results indicated that proliferative HCC patients with liver cirrhosis and larger tumor sizes were at high risk of recurrence after liver resection.[31–35] Notably, it is imperative to acknowledge that the prognosis of low-risk proliferative HCC is comparable to that of nonproliferative HCC, thus indicating that the treatment approach for these two subtypes could be the same. Interestingly, the lobulated shape of the tumor, the presence of satellite nodules, and high SII were closely associated with a worse prognosis in univariate analysis but not in multivariate analysis, which indicated these variables were confounding factors.

In the predictive analysis, the "CD" model and nomogram demonstrated outstanding accuracy in predicting the DFS of proliferative HCCs, with AUCs exceeding 0.7 for 1-, 3- and 5-year DFS in both the training and validation cohorts. The highlights of this study are as follows: first, compared with previous clinical studies on proliferative HCCs, such as Liu et al (nonproliferative HCC: n = 73; proliferative HCC: n = 82) and Kang et al (nonproliferative HCC: n = 106; proliferative HCC: n = 52), this study had a relatively larger sample size (nonproliferative HCC: n = 557; proliferative HCC: n = 259) and utilized PSM to validate that the prognosis of proliferative HCC was worse than that of nonproliferative HCC;[2,25] second, our study pioneered a relatively accurate, convenient, easily applicable, and relatively noninvasive method for predicting DFS in patients with proliferative HCC.

Despite the valuable results described above, there are several limitations in the present study that merit acknowledgment. Firstly, this was a retrospective study that was inherently susceptible to potential biases, especially the selection bias. In the process of analysis, parts of eligible patients were further excluded because of absence of baseline CT imaging within 1 month or unavailable baseline laboratory test results within 1 week before surgery, those exclusions may have introduced selection bias. Prospective studies encompassing a larger study cohort should be conducted to validate our observations. Secondly, the AUCs of the validation cohort were higher than that of the training cohort, which may be ascribed to the limited number of validation cohorts. Thirdly, due to the nature of retrospective study, there might be a time gap between the diagnosis of recurrence and the discovery of recurrence, and this may have an impact on the results. Fourth, our study was conducted in an area where the hepatitis B virus is endemic, while hepatitis B is not the primary cause of HCC in Europe or America. Consequently, our findings may not be generalizable to the global population. Therefore, further validation studies involving larger and more diverse patient cohorts are warranted to corroborate the clinical utility of this predictive model.

Conclusion

In summary, proliferative HCC exhibits a worse DFS compared with that of nonproliferative HCC. Proliferative HCC with liver cirrhosis and large tumor sizes were associated with high risk of recurrence, and a novel predictive model termed the "CD" model was developed herein for accurately predicting the prognosis of proliferative HCC. This predictive model may enhance individualized clinical management of proliferative HCC patients, thereby improving clinical outcomes.

Data Sharing Statement

Data is available upon reasonable request from Tian-Cheng Wang.

Acknowledgments

Disclosure

The authors report no conflicts of interest in this work.

References

1. Calderaro J, Ziol M, Paradis V, Zucman-Rossi J. Molecular and histological correlations in liver cancer. *J Hepatol*. 2019;71(3):616–630. doi:10.1016/j.jhep.2019.06.001
2. Kang HJ, Kim H, Lee DH, et al. Gadoxetate-enhanced MRI features of proliferative hepatocellular carcinoma are prognostic after surgery. *Radiology*. 2021;300(3):572–582. doi:10.1148/radiol.2021204352
3. Bao Y, Li JX, Zhou P, et al. Identifying proliferative hepatocellular carcinoma at pretreatment ct: implications for therapeutic outcomes after transarterial chemoembolization. *Radiology*. 2023;308(2):e230457. doi:10.1148/radiol.230457
4. Galle PR, Forner A, Llovet JM, et al. EASL clinical practice guidelines: management of hepatocellular carcinoma (vol 69, pg 182, 2018). *Correct J Hepatol*. 2019;70:182–236. doi:10.1016/j.jhep.2019.01.020
5. Heimbach JK, Kulik LM, Finn RS, et al. AASLD guidelines for the treatment of hepatocellular carcinoma. *Hepatology*. 2018;67(1):358–380. doi:10.1002/hep.29086
6. Reig M, Forner A, Rimola J, et al. BCLC strategy for prognosis prediction and treatment recommendation: the 2022 update. *J Hepatol*. 2022;76 (3):681–693. doi:10.1016/j.jhep.2021.11.018
7. Hwang S, Joh JW, Wang HJ, et al. Prognostic prediction models for resection of large hepatocellular carcinoma: a Korean multicenter study. *World J Surg*. 2018;42(8):2579–2591. doi:10.1007/s00268-018-4468-2
8. Ang SF, Ng ES, Li H, et al. The Singapore liver cancer recurrence (SLICER) Score for relapse prediction in patients with surgically resected hepatocellular carcinoma. *PLoS One*. 2015;10(4):e0118658. doi:10.1371/journal.pone.0118658
9. Chernyak V, Fowler KJ, Kamaya A, et al. Liver imaging reporting and data system (li-rads) version 2018: imaging of hepatocellular carcinoma in at-risk patients. *Radiology*. 2018;289(3):816–830. doi:10.1148/radiol.2018181494
10. Daniele B, Annunziata M, Barletta E, Tinessa V, Di Maio M. Cancer of the liver Italian program (CLIP) score for staging hepatocellular carcinoma. *Hepatol Res*. 2007;37(Suppl 2):S206–9. doi:10.1111/j.1872-034X.2007.00186.x
11. Chan EE, Chow PK. A review of prognostic scores after liver resection in hepatocellular carcinoma: the MSKCC, SLICER and SSCLIP scores. *Jpn J Clin Oncol*. 2017;47(4):287–293. doi:10.1093/jjco/hyw185
12. Kitao A, Matsui O, Zhang Y, et al. Dynamic CT and gadoxetic acid-enhanced MRI characteristics of p53-mutated hepatocellular carcinoma. *Radiology*. 2023;306(2):e220531. doi:10.1148/radiol.220531
13. Papageorge MV, de Geus SWL, Woods AP, et al. Surveillance patterns for hepatocellular carcinoma among screening-eligible patients in the medicare population. *Ann Surg Oncol*. 2022;29(13):8424–8431. doi:10.1245/s10434-022-12360-z
14. Borde T, Nezami N, Gaupp FL, et al. Optimization of the BCLC staging system for locoregional therapy for hepatocellular carcinoma by using quantitative tumor burden imaging biomarkers at MRI. *Radiology*. 2022;304(1):228–237. doi:10.1148/radiol.212426
15. Choi JH, Ro JY. Combined hepatocellular-cholangiocarcinoma: an update on pathology and diagnostic approach. *Biomedicines*. 2022;10(8):1826. doi:10.3390/biomedicines10081826
16. Yoon JK, Choi JY, Rhee H, Park YN. MRI features of histologic subtypes of hepatocellular carcinoma: correlation with histologic, genetic, and molecular biologic classification. *Eur Radiol*. 2022;32(8):5119–5133. doi:10.1007/s00330-022-08643-4
17. Hu B, Yang XR, Xu Y, et al. Systemic immune-inflammation index predicts prognosis of patients after curative resection for hepatocellular carcinoma. *Clin Cancer Res*. 2014;20(23):6212–6222. doi:10.1158/1078-0432.Ccr-14-0442
18. Smith A, Baumgartner K, Bositis C. Cirrhosis: diagnosis and management. *Am Fam Physician*. 2019;100(12):759–770.
19. van der PCB, McInnes MDF, Salameh JP, et al. CT/MRI and CEUS LI-rads major features association with hepatocellular carcinoma: individual patient data meta-analysis. *Radiology*. 2022;302(2):326–335. doi:10.1148/radiol.2021211244
20. Zafar F, Lubert AM, Trout AT, et al. Abdominal CT and MRI findings of portal hypertension in children and adults with Fontan circulation. *Radiology*. 2022;303(3):557–565. doi:10.1148/radiol.211037
21. Elder RW, McCabe NM, Hebson C, et al. Features of portal hypertension are associated with major adverse events in Fontan patients: the VAST study. *Int J Cardiol*. 2013;168(4):3764–3769. doi:10.1016/j.ijcard.2013.06.008
22. Nagtegaal ID, Odze RD, Klimstra D, et al. The 2019 WHO classification of tumours of the digestive system. *Histopathology*. 2020;76(2):182–188. doi:10.1111/his.13975
23. Tümen D, Heumann P, Gülow K, et al. Pathogenesis and current treatment strategies of hepatocellular carcinoma. *Biomedicines*. 2022;10(12):3202. doi:10.3390/biomedicines10123202
24. Dhondt E, Lambert B, Hermie L, et al. 90YRadioembolization versus drug-eluting bead chemoembolization for unresectable hepatocellular carcinoma: results from the trace phase ii randomized controlled trial. *Radiology*. 2022;303(3):699–710. doi:10.1148/radiol.211806
25. Liu G, Ma D, Wang H, et al. Three-dimensional multifrequency magnetic resonance elastography improves preoperative assessment of proliferative hepatocellular carcinoma. *Insights Imaging*. 2023;14(1):89. doi:10.1186/s13244-023-01427-4

26. Aoki T, Nishida N, Kudo M. Current perspectives on the immunosuppressive niche and role of fibrosis in hepatocellular carcinoma and the development of antitumor immunity. *J Histochem Cytochem*. 2022;70(1):53–81. doi:10.1369/00221554211056853

27. Liaskou E, Klemsdal Henriksen EK, Holm K, et al. High-throughput T-cell receptor sequencing across chronic liver diseases reveals distinct disease-associated repertoires. *Hepatology*. 2016;63(5):1608–1619. doi:10.1002/hep.28116

28. Moeini A, Torrecilla S, Tovar V, et al. An immune gene expression signature associated with development of human hepatocellular carcinoma identifies mice that respond to chemopreventive agents. *Gastroenterology*. 2019;157(5):1383–1397.e11. doi:10.1053/j.gastro.2019.07.028

29. Li HZ, Liu QQ, Chang DH, et al. Identification of NOX4 as a new biomarker in hepatocellular carcinoma and its effect on sorafenib therapy. *Biomedicines*. 2023;11(8):2196. doi:10.3390/biomedicines11082196

30. Kwag M, Choi SH, Choi SJ, Byun JH, Won HJ, Shin YM. Simplified LI-RADS for hepatocellular carcinoma diagnosis at gadoxetic acid-enhanced MRI. *Radiology*. 2022;305(3):614–622. doi:10.1148/radiol.220659

31. Yeh CN, Chen MF, Lee WC, Jeng LB. Prognostic factors of hepatic resection for hepatocellular carcinoma with cirrhosis: univariate and multivariate analysis. *J Surg Oncol*. 2002;81(4):195–202. doi:10.1002/jso.10178

32. Wee IJY, Moe FNN, Sultana R, et al. Extending surgical resection for hepatocellular carcinoma beyond Barcelona clinic for liver cancer (BCLC) stage a: a novel application of the modified BCLC staging system. *J Hepatocell Carcinoma*. 2022;9:839–851. doi:10.2147/jhc.S370212

33. Bae JS, Lee JM, Jeon SK, et al. LI-RADS Tumor in Vein at CT and Hepatobiliary MRI. *Radiology*. 2022;302(1):107–115. doi:10.1148/radiol.2021210215

34. Tay BWR, Huang DQ, Mark M, et al. Comparable outcomes in early hepatocellular carcinomas treated with trans-arterial chemoembolization and radiofrequency ablation. *Biomedicines*. 2022;10(10):2361. doi:10.3390/biomedicines10102361

35. Tong Y, Li JX, Chang DH, et al. An integrated liver function, systemic inflammation, and tumor characteristic score predicts prognosis in hepatocellular carcinoma after curative resection. *Ann Surg Oncol*. 2023;30(4):2007–2020. doi:10.1245/s10434-022-12899-x